J. Highw. Transp. Res. Dev. 2026, 20(1): 56−66

Journal of Highway and Transportation Research and Development

Home page: www.sciopen.com/journal/2095-6215

Consolidation characteristics of permafrost foundational soil in Yellow River source along G214

Jianhua Yu[*], Lei Quan[**], Bo Tian, Lihui Li, Panpan Zhang, Sili Li

Research Institute of Highway Ministry of Transport, Beijing, 100088, China

Abstract: This study conducted indoor consolidation tests on the aging road and natural ground foundational soils from the G214 permafrost section in the Yellow River source area to compare their consolidation characteristics. The results revealed that the consolidation deformation of the aging road foundation soil was significantly lower than that of the natural foundation soil, with a flatter consolidation curve. In the aging road foundation, the 2.5-4.3 m soil layer affected by annual temperature fluctuations exhibited void ratio variations 2.05 times greater than other layers. However, the variation in void ratio in multiple layers of the natural foundation was greater than that in the aging road foundation. The maximum settlement of the aging road foundation originated from the 2.5-4.3 m layer with smaller shallow settlement, while the natural foundation showed dominant shallow settlement followed by the 2.5-7.5 m layer, reaching a total settlement 1.37 times that of the aging road foundation. A layered treatment strategy is recommended: applying techniques adapted from soft foundation treatment to shallow layers while implementing thermal stability protection for permafrost in deeper layers, achieving a coordinated approach between deformation control and permafrost environmental protection.

Keywords: road engineering; consolidation characteristics; consolidation testing; permafrost; porosity ratio; foundation treatment

1 Introduction

Permafrost is an important engineering feature of highways in the Qinghai-Tibet Plateau region. The section of G214 route from Gonghe to Yushu, situated on the eastern edge of the Qinghai-Tibet Plateau's permafrost zone, constitutes a major permafrost highway traversing this area. The segment from Wenquan to Qingshuihe River spans over 200 km across permafrost terrain, characterized by high ground temperatures and substantial ice content [1−2]. Particularly, in most parts of this route, the permafrost is in a state of severe degradation [3]. Initially, it was believed that subsidence of the permafrost roadbed was solely due to thawing of the permafrost. However, subsequent studies revealed that this deformation is caused by multiple sources [4−6]. Researchers such as Tian Yahu [7] and Zhang [8] observed that the subsidence deformation of the embankment exhibits significant seasonal variations, with more pronounced seasonal deformations in high embankments. These deformations are concentrated in the warm season, while virtually no progression is noted during the cold season. Qi [9] suggest that the primary causes of roadbed subsidence in permafrost regions are thaw settlement, high-temperature permafrost, seasonal thaw creep, and additional deformations induced by freeze-thaw cycles under the influence of roadbed loads. Based on field subsidence monitoring and numerical simulation results, scholars such as Wang [10], Ma [11], and Yuan [12] assert that deformations during the operational phase of the highway are primarily concentrated within 0-7 m below the surface, mainly due to permafrost degradation and compressive consolidation. Sukai [13] found that high-temperature permafrost exhibits significant compressibility, but whether its deformation mechanism is creep or consolidation remains a topic of debate. Yu [5] and Ming [14] argue that the consolidation process in permafrost lags behind the thawing process and that the volume of consolidation deformation is generally substantial. This aspect of deformation warrants significant attention as newly thawed soil layers are unable to consolidate within the same year, requiring additional time for residual consolidation [15]. Further studies, such as those by Zhang, et al. [16] on the permeability coefficient of frozen Qinghai loess under load, suggest the possibility of consolidation in high-temperature permafrost. Liu and others [17] believe that the physico-mechanical properties of high-temperature permafrost are similar to those of thawed soil, thus justifying the use of consolidation theory to explain the deformation mechanisms of high-temperature permafrost.

Current foundation treatment technologies for permafrost areas mainly focus on protective treatment, forming a variety of technical solutions aimed at heat insulation, cold conduction, and water control [18]. However, under the influence of climate warming and humidification, large-scale uneven subsidence damage still occurs in the roadbeds of highways in permafrost areas [18]. During the operational lifespan of aging roads, the foundational soil beneath roadbeds undergoes significant degradation due to the coupled long-term effects of various additional stresses, including those from

Received: 14 May 2025; **Revised:** 20 June 2025; **Accepted:** 27 July 2025

[*] *E-mail address*: q949108627@gmail.com; [**] *Corresponding author*: b.tian@rioh.cn

DOI: 10.26599/HTRD.2026.9480084

Translated from Journal of Highway and Transportation Research and Development (Chinese, ISSN1002-0268), 2024, 41(S1):118−128.

RESEARCH INSTITUTE OF HIGHWAY MINISTRY OF TRANSPORT | SciOpen

permafrost. Over time, the pore water within the foundational soil is progressively expelled and dissipates, leading to the migration and reorganization of the pore structure and the soil's skeletal framework [19]. These alterations in the mechanical properties of the foundational soil result in changes under the influence of these forces, thereby impacting the stability of the roadbed. Analyzing the consolidation characteristics of the foundational soil in aging roads assists in assessing their long-term stability and provides essential references for reconstruction or reinforcement efforts. In contrast, natural foundational soil, which has not been subjected to such additional stresses, displays significantly different mechanical properties. The consolidation characteristics of natural foundational soil are greatly influenced by construction conditions, yet they can be enhanced through optimized design and construction processes, such as compaction and reinforcement, to achieve better consolidation effects. For the design and construction of new roads, understanding the consolidation characteristics of natural foundational soil helps reduce settlement and enhance the stability of the roadbed. During the operational period of newly constructed roads, the properties of the subgrade soil will gradually approach those of the existing road subgrade soil. Therefore, when designing foundations in permafrost regions, it is crucial to consider both thaw settlement and consolidation effects to ensure the long-term stability and safety of the engineering project.

This study focuses on the native soil samples from the permafrost section along the G214 route in the Yellow River Source of the Qinghai-Tibet Plateau as the subject of investigation. Through consolidation tests, we analyze the consolidation behavior of both aging and natural foundational soils at varying depths. The aim is to uncover the mechanical evolution patterns of foundational soil in permafrost regions in depth, thereby providing theoretical and technical support for the design and construction of new roads, as well as for the optimization of existing road upgrades in the Qinghai-Tibet Plateau permafrost areas.

2 Sampling and testing methodologies for foundational soil

2.1 Overview of the sampling area for foundational soil

The section of the Feldspar Mountain-Duoqin Ankelang area encompasses the longest stretch of continuous permafrost on G214 route, spanning 46.7 km between K417+200 and K463+900. Characterized by a high ice content, this permafrost segment accounts for 69.8% of the total permafrost length in the area, extending over 32.6 km. The average annual ground temperature ranges between −1.0 ℃ and −0.5 ℃, classifying it as high-temperature unstable permafrost. The average downward displacement rate of the natural upper limit of permafrost over many years and the average downward displacement rate of the upper limit of permafrost over many years after the construction of new roadbed pavement structures are 0.099 and 0.122 m/a, respectively [3]. The average temperature of this section ranges from −5.3 to −2.4 ℃, with an overall warming trend and a warming rate of approximately 0.2 ℃/(10a) [20]. The predominant soil types in this region are loamy sand and silty clay, which are fine-grained soils. Overall, the geotechnical conditions for permafrost engineering are relatively poor, with some road sections being in extremely poor condition [20]. The soil samples for this study were collected from the Feldspar Mountain-Duoqin Ankelang plains within the pile number range of K435+000 to K437+000 during the warm season of the permafrost region. The depth of the permafrost upper limit beneath the aging road's foundational soil reaches up to 9.0 m. The G214 highway from Gonghe to Yushu was widened and completed between 2001 and 2003, with an asphalt concrete surface, has experienced various degrees of pavement damage due to the permafrost effects. Following surface treatments in 2008, which included the application of a 4 cm thick asphalt concrete overlay, this section continues to suffer from numerous roadway defects, leading to a generally poor overall condition.

2.2 Stratification of foundational soil layer

To investigate the mechanisms by which road operations affect permafrost foundations, field drilling was conducted to collect undisturbed soil samples from beneath the centerline of the aging road and 1.5 m outside the toe of the same cross-section for foundational soil analysis. The sampling depths ranged from 0 to 7.4 m. The centerline of the aging road directly bears the heaviest vehicle loads and additional stresses on the pavement structure. It is located in the core area of the roadbed fill and is subject to the most severe disturbance. The natural foundation 1.5 m outside the toe of the slope in the same cross-section can effectively avoid the disturbance of the soil caused by road construction and operation and maintenance. At the same time, it can ensure that the sampling point and the centerline sampling point are in the same geological structure, hydrological conditions, and climatic environment. After collection, the samples were transported to the Ministry of Transport's Permafrost Observation Base for subsequent consolidation testing.

Based on the borehole data (refer to Fig. 1), apparent soil properties, and particle size distribution results, the foundational soil was classified into five distinct layers. These are detailed as follows: from 0 to 1.5 m, the layer consists of clayey fine sand; from 1.5 to 2.5 m, it comprises medium sand, which is unsuitable for consolidation tests; from 2.5 to 4.3 m, it consists of fine-grained soil; from 4.3 to 6.0 m, it includes clayey sand; and from 6.0 to 7.5 m, it consists of silty clay.

Fig. 1 Distribution of soil samples from field boreholes.

Soil samples were collected from the median depths of each soil layer to facilitate a clear visual demonstration of the soil layer properties and to aid in the subsequent analysis of soil sample testing results. The samples of foundational soil were systematically numbered. Table 1 presents the basic properties and sample identification for foundational soil.

2.3 Methodology for the consolidation test of foundational soil

The experimental apparatus employed in this study was a lever-action high-pressure consolidation instrument (Model WG single-lever consolidation apparatus, refer to Fig. 2). Prior to conducting the experiments, the equipment was meticulously calibrated to ensure that it was positioned on a level surface and the lever was balanced in a no-load condition. The method adopted for the experiment was the rapid consolidation technique, utilizing an undisturbed soil sample with a cross-sectional area of 30 cm^2 and a height of 2 cm. The samples, including those from an aging road foundational soil and natural foundational soil, were subjected to high-pressure consolidation tests under double-sided drainage conditions, with incremental loading applied.

To explore the thawing process of permafrost in natural foundational soil subsequent to roadbed construction, the tests were con-

Table 1 Basic properties of foundational soil samples.

Foundation soil samples	Number	Sampling layer (m)	Apparent properties	Initial porosity ratio	Density (g/cm^3)	Moisture content (%)	Dry density (g/cm^3)
Aging road foundational soil samples	A1	0-1.5	Clayey fine sand	0.65	1.78	8.70	1.63
	A2	2.5-4.3	Fine-grained soil	0.70	1.99	23.77	1.61
	A3	4.3-6.0	Clayey sand	0.48	2.20	19.18	1.85
	A4	6.0-7.5	Silty clay	0.47	2.14	15.21	1.86
Natural foundational soil samples	B1	0-1.5	Clayey fine sand	0.74	2.02	23.6	1.55
	B2	2.5-4.3	Fine-grained soil	0.60	2.12	22.8	1.70
	B3	4.3-6.0	Clayey sand	0.51	2.10	17.1	1.79
	B4	6.0-7.5	Silty clay	0.54	2.12	21.9	1.74

Fig. 2 Field consolidation test of foundational soil.

ducted under local climatic conditions (10 °C, 0.6 atm pressure). Each load level was maintained for a duration of 1 h, and readings were taken at the final load level until settlement stabilized. The criterion for consolidation stability was defined as a deformation of no more than 0.01 mm in the final hour. The test loads were sequentially set at 25, 50, 100, 200, 400, 800, and 1,600 kPa, with timing intervals recorded at 0.25, 1, 2.25, 4, 6.25, 9, 12.25, 16, 20.25, 25, 30.25, 36, 42.25, and 60 min.

3 Experimental results and analysis

3.1 Consolidation compression characteristics of foundational soil in aging roads

3.1.1 Consolidation curve of foundational soil in aging roads

Fig. 3 shows the consolidation settlement curves of the aging road foundation soil at different depths. As the consolidation tests progressed, the consolidation settlement curves of soil samples at various depths gradually flattened out, exhibiting typical consolidation settlement characteristics: an initial rapid compression phase, an intermediate deceleration phase, and a final stabilization phase. During the initial stage, soil samples from all depths of the aging road foundation exhibited a noticeable rapid increase in settlement. As time progressed, the settlement rate significantly slowed, and the consolidation rate gradually decreased. Ultimately, the curves stabilized, with minimal changes in settlement, indicating that the consolidation process had largely concluded. The consolidation deformation of the A1 soil sample was the smallest among all aging road foundation soil samples, with relatively slow changes in settlement throughout the loading stage. In contrast, the consolidation deformation of the A2 soil sample was significantly higher than that of other soil samples, making it the largest deformation among all aging road foundation soil samples. Additionally, the deformation of the A3 and A4 soil samples was also relatively large but slightly lower than that of the A2 soil sample.

3.1.2 Compressive characteristics of the aging road's foundational soil

As depicted in Fig. 4, the compressive characteristics of the foundational soil from an aging road were obtained through the one-dimensional consolidation test. This test yielded the e-lg p curves for four undisturbed soil samples from the foundational layer. During the consolidation process, the trends in porosity ratio changes under various loads were consistent across all soil samples. The porosity ratio (e) of each sample decreased progressively with increasing pressure. The curve profiles for samples at different depths were similar, exhibiting an inverse relationship. When comparing samples from different depths, it was observed that the initial porosity ratio decreased with increasing depth. Specifically, soil samples A1 and A2 exhibited significantly higher initial porosity ratios than samples A3 and A4. As indicated in Table 1, the initial porosity ratio for sample A1 was 0.65, slightly lower than that of A2, yet demonstrating greater compressibility. The initial porosity ratio of sample A2 was the highest among the samples at 0.70, and it showed a substantial decrease in porosity ratio during consolidation, approximately 2.05 times greater than other layers. In contrast, the deeper samples (A3 and A4) had lower initial porosity ratios of approximately 0.48 and 0.47, respectively, indicating that the deeper soil layers were more compact and less compressible.

3.2 Consolidation characteristics of natural foundational soil

3.2.1 Consolidation curve of natural foundational soil

Fig. 5 shows the consolidation settlement curves for natural foundation soils at different depths. As the consolidation test time increases, the consolidation settlement curves for soil samples at various depths gradually become flatter, exhibiting typical consolidation settlement characteristics: an initial rapid compression phase, an intermediate deceleration phase, and a final stabilization phase. During the initial stage, soil samples from all depths exhibit a noticeable rapid increase in settlement. As time progresses, the settlement rate significantly slows down, and the consolidation rate gradually decreases. Ultimately, the curves stabilize, with minimal changes in settlement, indicating that the consolidation process has largely concluded. Soil samples at different depths exhibit similar trends under the same pressure conditions. Among them, B1 and B4 soil samples exhibit greater deformation during consolidation, indicating stronger compressibility, while B2 and B3 soil samples exhibit smaller deformation and lower compressibility. This indicates that shallow and deep soils exhibit faster and more intense deformation responses, while intermediate-depth soils exhibit smaller deformation amplitudes and rates. This suggests that depth has a significant influence on the consolidation characteristics of soil.

3.2.2 Compressive characteristics of natural foundational soil

As depicted in Fig. 6, the compressibility of four groups of undisturbed natural foundational soil samples was assessed through one-dimensional consolidation tests. These tests yielded the e-lg p curves for each soil sample.

Overall, during the consolidation process, the trend in the change of porosity ratios under varying loads was consistent across all samples. As pressure increased, the porosity ratio (e) of all samples decreased progressively, indicating a negative correlation. The shape of the curves for samples from different depths was similar, suggesting uniform behavior across the sample depths. A comparative analysis of samples from various depths reveals that the ini-

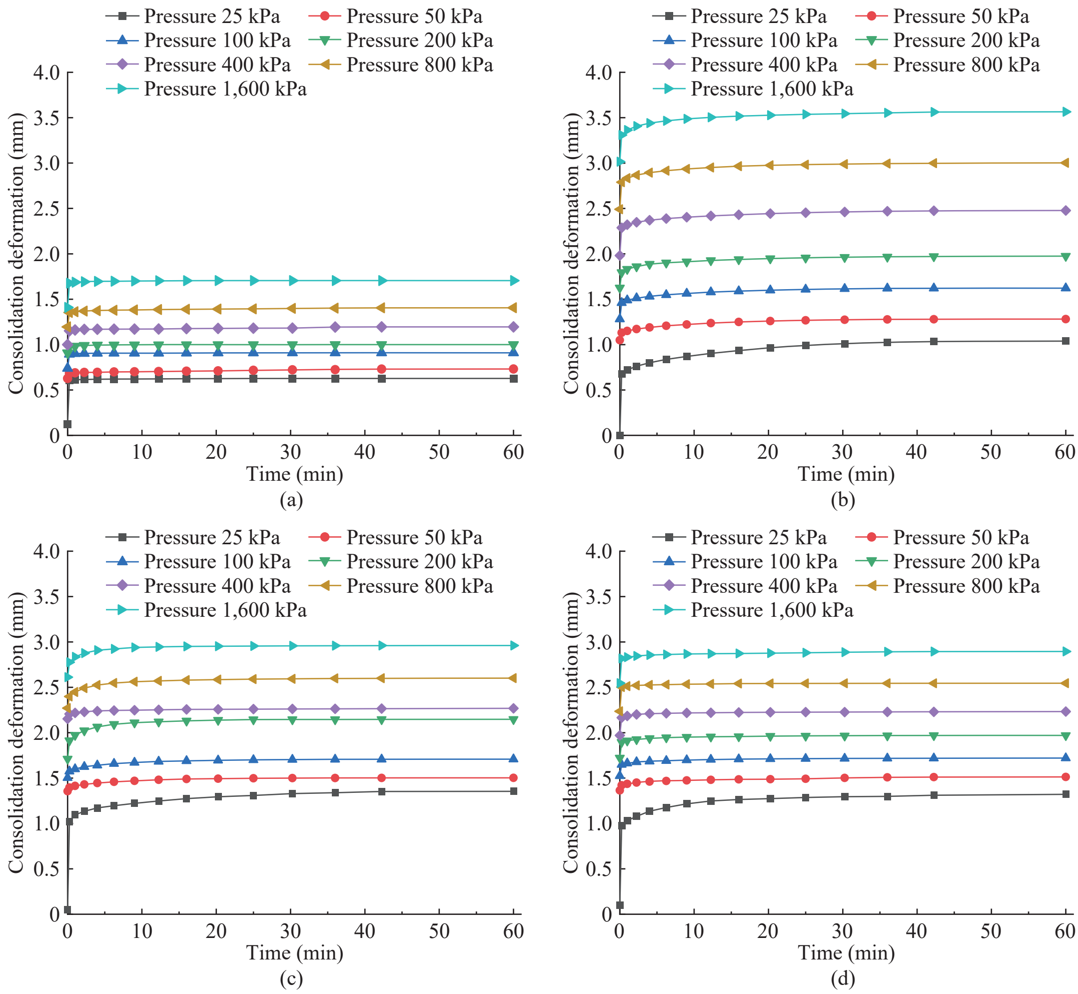

Fig. 3 Settlement curves for consolidation of foundational soil on aging roads at various depths. (a) Consolidation settlement curve for soil sample A1. (b) Consolidation settlement curve for soil sample A2. (c) Consolidation settlement curve for soil sample A3. (d) Consolidation settlement curve for soil sample A4.

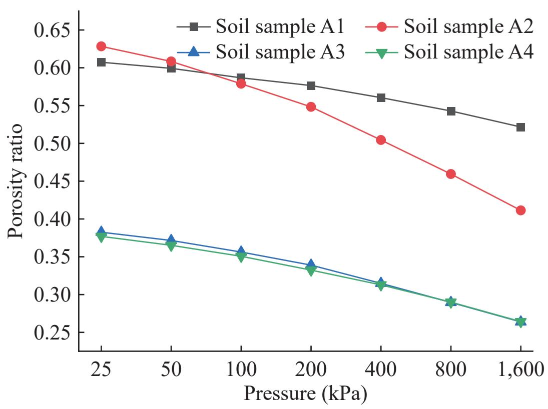

Fig. 4 Void ratio-pressure relationship of existing road subgrade soil.

tial porosity ratio decreases with increasing depth of sampling. According to Table 1, the initial porosity ratios of shallower samples are significantly higher than those of deeper samples. Specifically, Sample B1, with an initial porosity ratio of 0.74, exhibited the highest initial porosity among the natural foundational soil samples, indicating a loose arrangement of particles and a higher porosity in the shallower strata. Under increasing pressure, Sample B1 showed the greatest reduction in porosity ratio, highlighting the marked compressibility of shallow soil under high pressure. Sample B2 had an initial porosity ratio of approximately 0.60, slightly lower than that of B1, yet it still demonstrated considerable compressibility and a deformation pattern similar to that of B1. In contrast, the mid to deep layer samples (B3 and B4) had lower initial porosity ratios, approximately 0.51 and 0.54 respectively, suggesting that the deeper soil strata are more densely packed and exhibit lower compressibility. Notably, Sample B4 maintained the lowest porosity ratio throughout the loading process.

3.3 Comparative study on the compression characteristics of consolidation

3.3.1 Comparison of consolidation characteristics

Fig. 7 illustrates the comparative total settlement due to consolidation of foundational soil from various depths of an aging road with that of natural foundational soil. The results indicate significant differences in the settlement volumes of soil samples at different depths. Between depths of 0 to 1.5 m, the consolidation deformation of natural foundational soil (B1) significantly exceeds that of the aging road foundational soil (A1). At depths of 2.5 to 4.3 m, the consolidation deformation of the aging road foundational soil (A2) surpasses that of the natural foundational soil (B2). Between 4.3 to 6.0 m, the settlement volumes of both types of soil are comparable, though the natural foundational soil (B3) shows slightly higher settlement, suggesting similar physical properties within this depth range. From 6.0 to 7.5 m, the consolidation deformation of the natural foundational soil (B4) is greater than that of the aging road foundational soil (A4). Overall, the natural foundational soil exhibits significantly higher settlement volumes at both

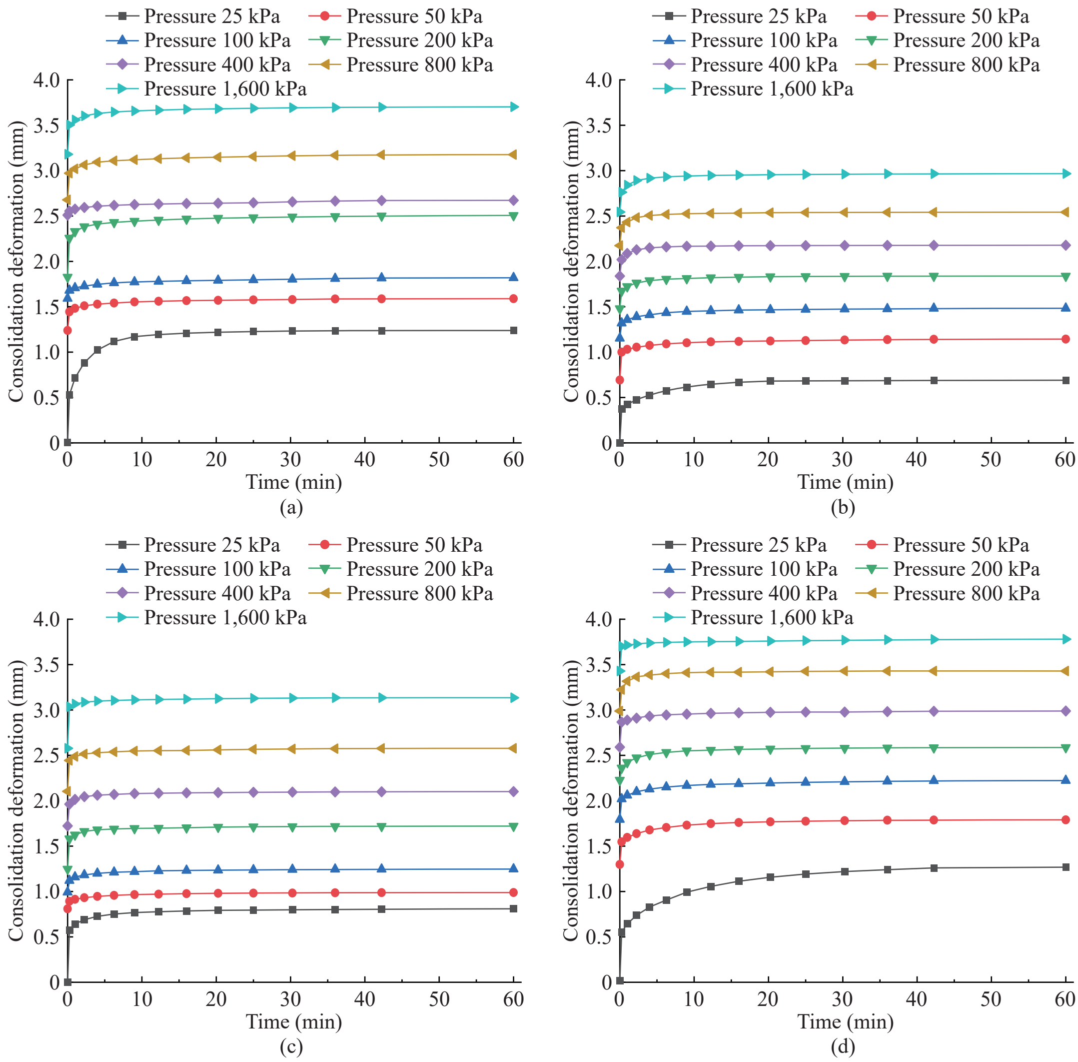

Fig. 5 Consolidation settlement curves of natural foundational soil at various depths. (a) Consolidation settlement curve for soil sample B1. (b) Consolidation settlement curve for soil sample B2. (c) Consolidation settlement curve for soil sample B3. (d) Consolidation settlement curve for soil sample B4.

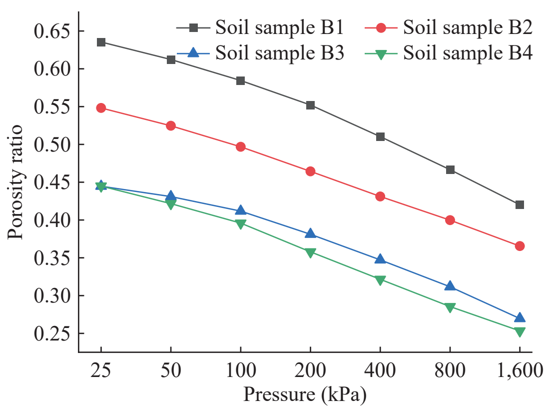

Fig. 6 Void ratio-pressure relationship of Natural foundation soil.

shallow and deep layers compared to the aging road foundational soil, whereas the latter shows higher settlement at intermediate depths.

Based on the consolidation curves, the coefficient of consolidation can be calculated using the square root of time method. After determining the time, t_{90}, when the degree of consolidation reaches 90%, the coefficient of consolidation C_v can be computed as follows:

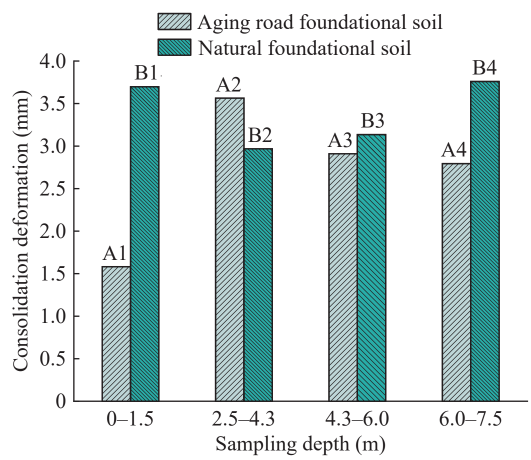

Fig. 7 Consolidation settlement comparison.

$$C_{\mathrm{v}} = \frac{0.848\bar{h}^2}{t_{90}} \tag{1}$$

$$\bar{h} = \frac{h_1 + h_2}{4} \tag{2}$$

where, C_v is coefficient of consolidation (cm^2/s); $\bar{h}$ is Half the average of the initial and final heights of the sample under a specific load.

As demonstrated in Fig. 8, both the foundational soil samples from aging roads and those from natural conditions exhibit a decreasing trend in the coefficient of consolidation as the consolidation pressure increases. Specifically, for the foundational soil samples from aging roads, Sample A1 displays the highest coefficient of consolidation. Samples A3 and A4 exhibit similar coefficients under low load conditions; however, under higher load conditions, the coefficient for Sample A4 exceeds that of Sample A3. Sample A2 shows the slowest rate of consolidation, indicating that the 0 to 1.5 meter soil samples from aging roads consolidate more rapidly, requiring less time to achieve full consolidation. In contrast, the 2.5 to 4.3 m soil samples from aging roads demonstrate a slower rate of consolidation and consequently require a longer period to consolidate. Regarding the natural foundational soil samples, Sample B3 presents the highest coefficient of consolidation. Other samples in this category show similar consolidation coefficients under low load conditions, but under higher loads, the coefficient for Sample B1 is greater than those for Samples B2 and B4. A comparison of the consolidation curves from the same stratigraphic levels in Fig. 8 panels (a) and (b) reveals that at equivalent loading conditions, the consolidation coefficients for the 0 to 1.5 m and 6.0 to 7.5 m soil samples from aging roads are higher than those for the natural foundational soils. Conversely, the consolidation coefficients for the 2.5 to 6.0 m soil samples from aging roads are lower than those for the corresponding natural foundational soils.

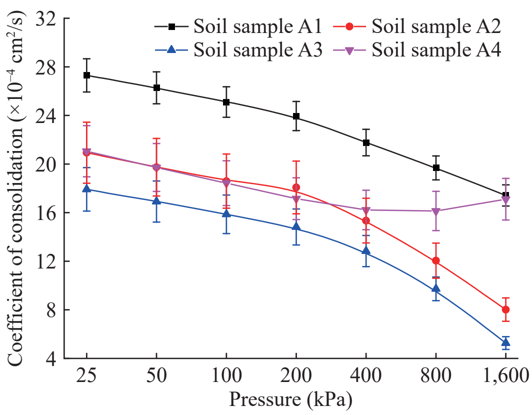

(a)

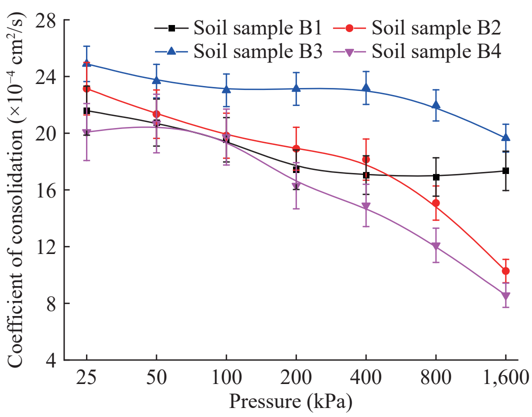

(b)

Fig. 8 Relationship between C_v and p for undisturbed foundational soil samples.
(a) C_v-p Relationship curve for aging road foundational soil sample.
(b) C_v-p Relationship curve for natural foundational soil sample.

3.3.2 *Comparative analysis of compression characteristics*

Fig. 4 and Fig. 6 reveal that the $e-\lg p$ curves for the foundational soil of the aging road and the natural foundational soil exhibit a similar overall trend. Specifically, both demonstrate a characteristic reduction in the porosity ratio as the load increases. Excluding the soil layers between 2.5 and 4.3 m, the initial porosity ratios of the foundational soil from the aging road at various depths are generally lower than those of the natural foundational soil. Notably, in the soil layers between 4.3 and 7.5 m, the initial porosity ratio of the foundational soil from the aging road is significantly lower than that of the nearby natural foundational soil. As shown in Fig. 9, with the exception of the 2.5 to 4.3 m layers, the amplitude of porosity ratio changes in the natural foundational soil exceeds that in the foundational soil of the aging road. The initial porosity ratios of soil samples A2 and B2 are approximately 0.70 and 0.60, respectively, with A2 exhibiting a higher porosity ratio than B2. Furthermore, post-loading changes in the porosity ratio are more pronounced for sample A2 compared to B2, indicating a more significant compressibility in the foundational soil of the aging road between 2.5 and 4.3 m.

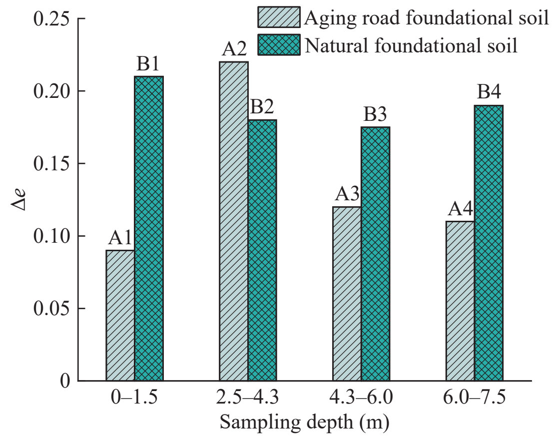

Fig. 9 Comparison of variation in porosity ratio.

Further data processing of the $e-\lg p$ curves allows for the calculation of pre-consolidation pressure and average overlying pressure at different depths, which in turn facilitates the calculation of the pre-consolidation ratio *OCR* and obtaining the over consolidation characteristics of foundation soil, The results are shown in Table 2.

Table 2 Super-consolidation characteristics of road foundational soil

Soil sample number	Pre-consolidation pressure (kPa)	Average overlying pressure (kPa)	*OCR*
A1	69.2	17.8	3.90
A2	61.6	75.6	0.81
A3	70.5	114.4	0.62
A4	183	145.3	1.26
B1	25.1	8.1	3.10
B2	35.4	84.8	0.42
B3	83.2	100.8	0.82
B4	79.5	148.4	0.54

As shown in Table 2, the foundational soil samples A1 and A4 from the aging road segment through the permafrost regions of the G214 Yellow River source exhibit notably high *OCR* values, indicating a state of over-consolidation. Conversely, samples A2 and A3 are characterized by under-consolidation, approaching a normal consolidation state. In contrast, the natural foundational soils display generally lower OCR values at various depths, particularly samples B2 and B4, where the *OCR* values are significantly below 1, indicative of an under-consolidated state. The pre-consolidation pressure of the foundational soil from the aging road is consistently higher than that of the natural foundational soil. This discrepancy can be attributed to the aging road foundation enduring long-term exposure to various loads such as the weight of the roadbed itself, operational loads, and additional imposed loads, which have facilitated considerable consolidation. In comparison, the consolidation in natural foundational soils is primarily influenced by their self-weight, resulting in relatively weaker consolidation effects.

3.3.3 Verification through static cone penetration test and differential analysis

Previous studies have shown that the cone penetration test (CPT) is effective in assessing the bearing characteristics of active layers in permafrost areas [21]. During the analysis of Figs. 5 to 7, a special layer (2.5 to 4.3 m) was found in the aging road foundation soil, which was significantly different from other layers. Therefore, the cone penetration test was used for verification. Fig. 10 shows the in-situ static cone penetration test results for the aging road foundation and the natural foundation. According to relevant literature [21], the standard for determining the bearing layer of the foundation in permafrost areas based on CPT tests is a cone tip resistance of 8 MPa. When the cone tip resistance exceeds 8 MPa, the soil has strong bearing capacity and can serve as the bearing layer. Therefore, the depth range where the cone tip resistance is ≤8 MPa can be identified as a weak layer. As shown in Fig. 10, the cone tip resistance within the 0 to 4.8 m depth range of the road subgrade soil is below 8 MPa, failing to meet the criteria for a bearing layer. Although the natural subgrade soil at the same depth interval has local sections with values greater than 8 MPa, the average value between layers is still below 8 MPa, and its overall cone tip resistance is significantly higher than that of the aging road subgrade soil. This indicates that after the construction of the frozen soil subgrade, the additional loads encountered during road operation have significantly degraded the mechanical properties of the subgrade soil, leading to a decline in bearing capacity under the combined thermal-mechanical effects. Notably, the cone tip resistance and lateral friction resistance in the 2.0 to 4.0 m interval of the aging road foundation soil exhibit abnormally low values, while the two parameters in the natural foundation soil show a relatively uniform overall distribution, with only narrow low-value intervals in localized areas. Based on this, it is inferred that the 2.0 to 4.0 m layer is the most sensitive soil layer subjected to the most severe disturbance under thermal-mechanical coupling effects in the aging road foundation.

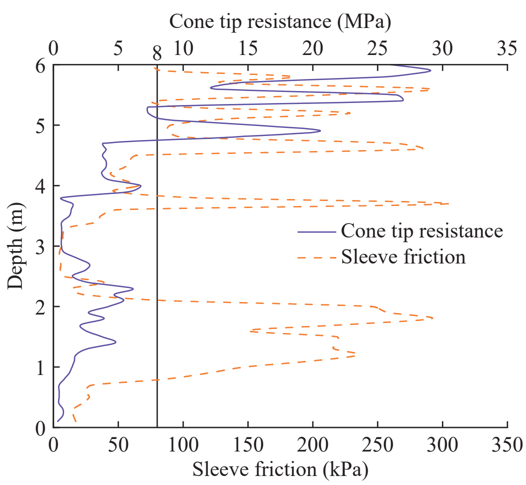

(a)

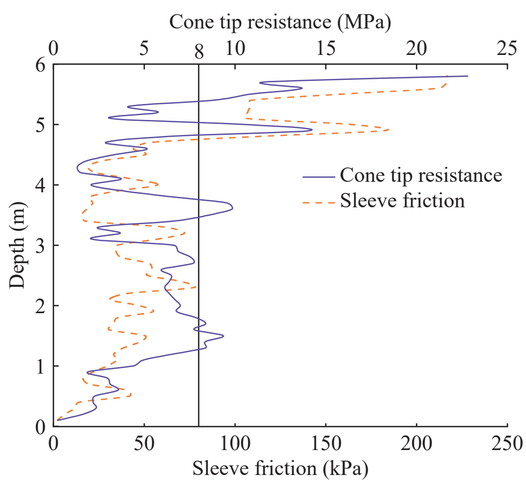

(b)

Fig. 10 In-situ static cone penetration test results. (a) In-situ static cone penetration test results for the aging road foundational soil. (b) In-situ static cone penetration test results for the natural foundational soil.

To investigate the cause of the significantly low static cone penetration resistance and sidewall friction in the 2.0 to 4.0 m soil layer of the aging road foundation soil, and given that the geological distribution of the natural foundation and the aging road foundation is consistent with the distribution of groundwater, and considering the significant thermal disturbance effects caused by road embankment construction in permafrost regions, it is speculated that this anomaly is related to the redistribution of the foundation temperature field. To this end, the monitored temperature data of the aging road foundation soil were analyzed, with the results shown in Fig. 11). The results indicate that within a depth range of 0 to 2.0 m, temperature fluctuations are most pronounced. However, due to the direct impact of roadbed loads, the surface soil is sufficiently densified and compacted, resulting in minimal changes in consolidation deformation and porosity ratio. Between depths of 2.0 and 4.5 m, the soil temperatures fluctuate significantly, stabilizing at relatively high temperatures (near 0 °C) before the onset of the warm season (January to May), with a fluctuation range of 3 to 11 °C under the influence of thermal conductivity during the warm season. Below 4.5 m, the temperature variations are less pronounced. Consequently, it can be inferred that the soil layer between 2.0 and 4.5 m is subject to significant temperature fluctuations over the long term, influenced by freeze-thaw cycles, which lead to a loosening of the soil structure and a reduction in load-bearing capacity. The shallower layers, subjected to additional stress, exhibit reduced compressibility yet maintain a higher load-bearing capacity.

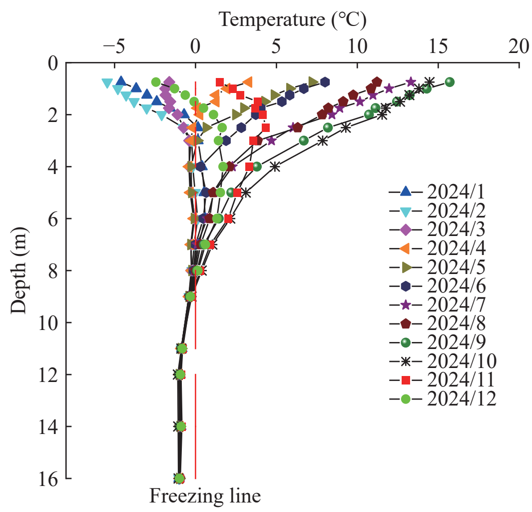

Fig. 11 Temperature data for the aging road foundational soil.

4 Foundation optimization strategies based on settlement characteristics

4.1 Prediction of foundation settlement

The layered summation method is a generic term for a category of settlement calculation methods. In these methods, the layers of foundational soil within the compression zone are divided into several strata, and the vertical compression of each stratified soil layer is calculated separately. The total settlement volume is then obtained by summing these individual compressions. This approach typically employs a one-dimensional compression model [22−23].

As depicted in Fig. 12, when the stress on the soil increases from P_1 to P_2, the height of the soil decreases from H_1 to H_2, and the porosity ratio changes from e_1 to e_2. Under these conditions, the volume change per unit of soil can be expressed as:

$$\frac{V_1-V_2}{V_1}=\frac{(1+e_1)V_s-(1+e_2)V_s}{(1+e_1)V_s}=\frac{e_1-e_2}{1+e_1} \tag{3}$$

where, V_1 is the volume of the sample before compression; V_2 is the volume of the sample after compression; and V_s is the volume of the soil.

From Eq. (3), the volumetric compression deformation of the soil unit, disregarding lateral deformation, can be described by:

$$\Delta z=\frac{e_1-e_2}{1+e_1}H=\frac{-\Delta e}{1+e_1}H \tag{4}$$

Experimental results can yield the soil compression curves ($e-p$ or $e-\lg p$) for a single layer, and the total settlement of an n-layer foundation is the sum of the compressions of each layer, expressed as:

$$S=\sum_{i=1}^{n}\Delta z_i=\sum_{i=1}^{n}\frac{-\Delta e_i}{(1+e_0)_i}z_i \tag{5}$$

where, Δz_i is the compression amount of the i-th layer of soil; z_i is the thickness of the i-th layer of soil; e_i is the porosity of the i-th layer of soil before compression; and Δe_i is the change in porosity of the i-th layer of soil.

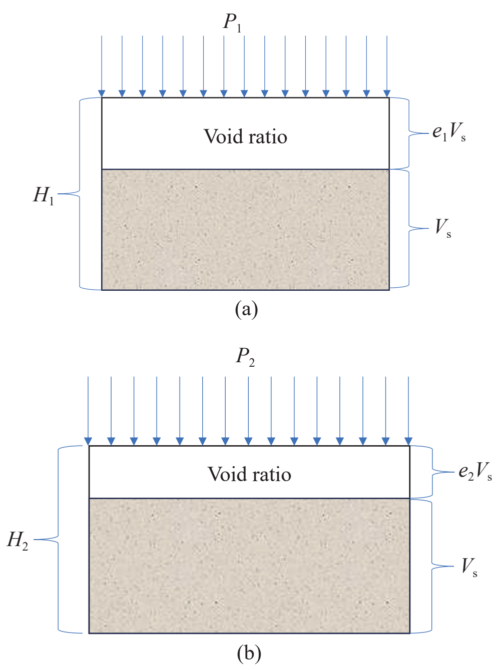

Fig. 12 Specimen before and after compression. (a) Condition of the sample before compression. (b) Condition of the sample before compression.

Assuming a uniform distribution of the soil layers in both natural foundational soil and the soil of an aging road foundation, the total deformation for both the natural and aging road foundations can be calculated using the above equation. Initial porosity ratios are selected as per Table 1, while the final porosity ratios are interpolated based on the stress levels sustained by the foundation. According to Eqs. (3) to (5), the total settlement volume of the aging road foundation is 313.5 mm, with the individual layer settlements being 58.9, 100.1, 82.4, and 72.12 mm for layers A1, A2, A3, and A4, respectively. The total settlement volume for the natural foundation is 429.6 mm, with individual layer settlements of 140.8, 100.1, 92.1, and 91.4 mm for layers B1, B2, B3, and B4, respectively. The total settlement of the natural foundation is approximately 1.37 times that of the aging road foundation. The settlement in the 0 to 1.5 m soil samples of the aging road foundation is relatively small due to the effects of prolonged loading, with the majority of settlement occurring below 2.5 m, particularly between 2.5 and 4.3 m contributing the most. In contrast, the settlement of the natural foundation is primarily concentrated in the 0 to 1.5 m and 2.5 to 4.3 m soil layers, with lesser settlement occurring in other layers.

4.2 Optimization of foundation treatment approaches

Previous research in the field of permafrost has introduced the design concept of “active cooling, cooling the foundation, and protecting permafrost” to maintain the stability of permafrost roadbeds. However, this concept is primarily applicable to railways or lower-grade roads that are less affected by thermal influences. Considering the potential impacts of future climatic changes on the Qinghai-Tibet Plateau and the degradation of permafrost, road engineering in this region still faces numerous challenges in terms of high-quality construction, maintenance, and disaster prevention and mitigation. Currently, the technologies for treating diseased permafrost roads can be categorized into three types: passive cooling of the foundation, active cooling of the foundation, and measures to enhance the permafrost foundation. The technologies of passive and active cooling foundations are relatively mature, centered around controlling the temperature increase of the foundation, slowing the occurrence of diseases, and protecting the permafrost. These technologies include high embankment roadbeds, insulation layer installation, improved fill materials, rubble roadbeds, ventilated roadbeds, and thermosyphon roadbeds [24]. While these technologies have alleviated roadbed diseases in permafrost areas to some extent, issues still persist in regions with significant thermal disturbances. Measures to enhance the permafrost foundation have been effectively applied in areas of isolated permafrost and seasonal frost regions, such as lime piles [25], replacement methods, and chemical improvement techniques [26]. In response to industry issues such as insufficient strength and uncontrollable deformation of degrading permafrost foundations, analogous approaches from soft soil foundation treatments and strategies to protect deep permafrost have been adapted. By integrating the characteristics of foundation settlement and deformation in permafrost areas, the selection and optimization of foundation treatment measures aim to improve the load-bearing capacity and deformation coordination ability of the permafrost foundation from multiple perspectives.

In the analysis of foundation settlement prediction, it was found that, regardless of whether it was an aging road foundation or a natural foundation, the main source of settlement was soil layers above 4.3 m. Therefore, the selection of foundation treatment plans should focus on techniques that effectively reinforce up to a depth of 4.3 m, while also considering those that can stabilize depths up to 7.0 m.

4.2.1 Dynamic consolidation technology for weak foundations

Dynamic consolidation is a method that utilizes intense compaction energy to generate impact forces, creating compression waves within the foundation which, in turn, strengthens the soil. As depicted in Fig. 13, when employing a tamper with a diameter of 2.0 m and an impact energy of 4 000 kN·m, the spacing between tamp points can be set at 3.5 m, achieving a displacement depth of 3.6 m and an effective consolidation depth of 8.0 m [27]. Given the effective depth of consolidation achieved by dynamic consolidation, it is observed that the effective consolidation depth during the thawing period exceeds that during the freezing period under the same energy level. Based on the design energy level of dynamic compaction, when the compaction energy level is low, it is advisable to conduct construction during the thawing period of the active layer. However, during this period, the bearing capacity of the active layer is low, making it difficult for heavy equipment to access the site, necessitating pre-reinforcement of the ground surface; When the compaction energy level is high, it is recommended to perform dynamic compaction during the freezing period. During this period, the surface soil layer is frozen, providing high bearing capacity, ensuring stable equipment operation, reducing the need for treatment procedures in weak active layers, and shortening the construction schedule [28]. Under the impact of dynamic consolidation, there are no significant changes in the longitudinal wave velocity of the soil, indicating minimal disturbance to the thermal field and negligible thermal shock disturbance to the permafrost.

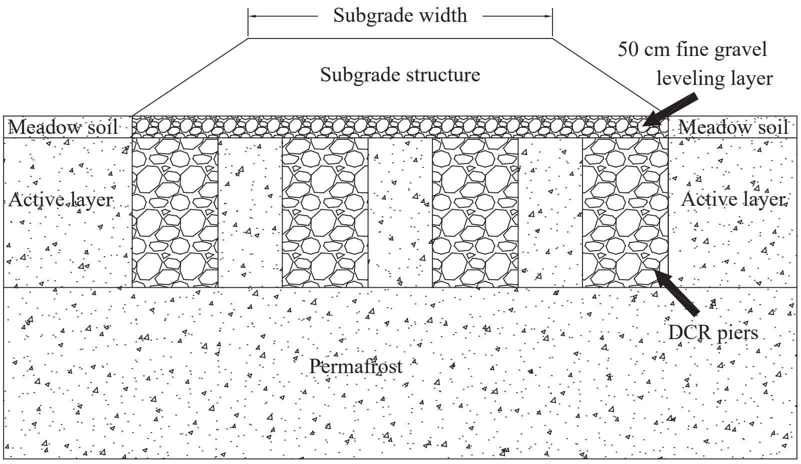

Fig. 13 Schematic diagram of dynamic compaction consolidation for weak foundation.

4.2.2 Rigid pile composite foundation technology

Rigid pile composite foundation technology is an ideal treatment for permafrost foundations. This technique involves driving the pile through the active layer and utilizing the stable underlying permafrost as a bearing stratum, thereby enhancing the foundation's load-bearing capacity and resistance to deformation (Fig. 14). Rigid pile composite foundations often use prefabricated piles, such as precast pipe piles and prestressed pipe piles. Not only does this technique improve the ability to coordinate deformation, reducing the risk of differential deformation due to thaw settlement beneath roads, it also utilizes the deep, stable permafrost as a bearing layer. This allows the superficial permafrost to degrade to some extent, adapting to the engineering context of a warming climate. The construction of rigid pile composite foundations is less constrained by surface bearing capacity. Its static pressure pile formation process can adapt to the weak bearing conditions of the surface soil layer during the thawing period. At the same time, the surface soil layer during the thawing period is easily penetrated by the piles, significantly improving pile driving efficiency and shortening the construction period. Therefore, this technology can be used for construction during the thawing period in permafrost areas.

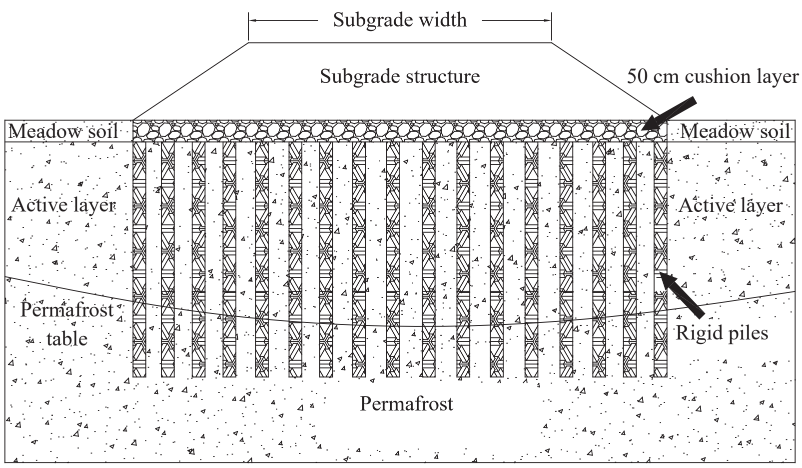

Fig. 14 Schematic diagram of rigid pile composite foundation technology.

4.2.3 Enhancement technology for shallow in-situ foundation solidification

The enhancement technology for shallow in-situ foundation solidification significantly improves the engineering properties of the soil in the active layer by utilizing in-situ solidification methods, thereby enhancing its load-bearing capacity and stability. The core of this technology involves using the in-situ foundational soil as the primary material, combined with suitable solidifying agents to improve the soil's chemical and physical properties (Fig. 15). Through the application of solidifying agents, not only is a high-strength artificial hard shell layer formed, but the permeability of the soil is also effectively reduced, minimizing moisture migration and subsequently lowering the water content of the shallow foundation. This process prevents volume changes caused by freeze-thaw cycles, reduces uneven deformations such as frost heave and settlement, and ensures the long-term stability and load-bearing capacity of the foundation. The shallow in-situ foundation solidification enhancement technology leverages natural soil as the main material, reducing costs associated with waste disposal, transportation, and backfilling, which is particularly advantageous in areas like the Qinghai-Tibet Plateau where transportation and backfilling are challenging. The enhancement technology for shallow in-situ foundation solidification requires soil excavation and backfilling operations. However, during the freezing period in permafrost regions, the high strength of the frozen surface impedes excavation efficiency. Therefore, construction should be scheduled during the thawing period when excavation is easier.

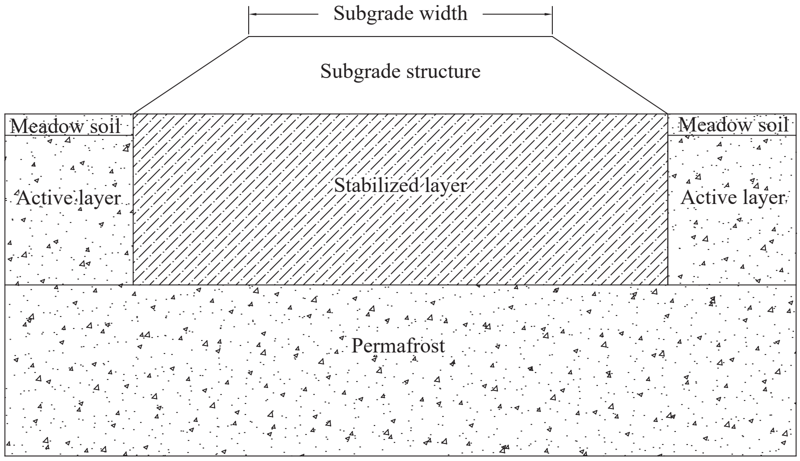

Fig. 15 Schematic diagram of shallow in-situ foundation solidification enhancement technology.

5 Conclusion

This study conducts an empirical investigation through indoor consolidation tests to study the compressive characteristics of foundational soil from both the natural ground and aging road sections along the G214 source area of the Yellow River's permafrost. It successfully extracts multiple parameters, including settlement volume, porosity ratio, pre-consolidation ratio, and consolidation coefficient, from different soil strata. The analysis not only distinguishes the consolidation behaviors at various depths between natural and aging road foundations but also verifies these behaviors through static cone penetration tests and on-site temperature monitoring, thereby providing an analytical basis for understanding the differential settlement characteristics. Our primary findings are summarized as follows:

(1) The initial porosity ratio of the foundational soil from the aging road base is generally lower than that of the natural ground, with a correspondingly higher consolidation ratio. Notably, the change in porosity during the consolidation process in the soil layers between 2.5 to 4.3 m in the aging road foundation is approximately 2.05 times that of other layers. Except for the 2.5 to 4.3 m layers, the natural ground foundation exhibits a generally higher porosity ratio change, indicating a stronger compressibility.

(2) The settlement volume of the aging road foundational soil is consistently less than that of the natural ground, especially under high load conditions, where the difference in settlement becomes more pronounced. The primary source of settlement in the aging road foundation is the 2.5 to 4.3 m soil layer, with the smallest settlement recorded in the 0 to 1.5 m layer; by contrast, the greatest settlement in the natural ground occurs in the 0 to 1.5 m layer, approximately 1.37 times that of the aging road foundation. Due to the combined effects of heat and force, the 2.0 to 4.0 m layer of the road during its operational period becomes the most sensitive soil layer subject to the most severe disturbance, and this layer requires special attention and treatment.

(3) In addressing settlement deformation characteristics within road engineering foundation projects, it is feasible to employ techniques such as dynamic compaction of weak foundations, rigid pile-composite foundation technology, and shallow in-situ foundational solidification enhancement. These measures are aligned with both soft soil foundation treatment schemes and deep permafrost preservation strategies.

(4) Our research reveals that permafrost areas possess a significant distribution of groundwater within the thawing layers, and the thermohydraulic coupling effects under a warming and humidifying environmental backdrop are non-negligible. Considering these factors comprehensively, future developments could focus on an integrated disease treatment technology that strengthens shallow foundations, protects deep permafrost, and manages water comprehensively.

Acknowledgments

None.

Funding

This research The study is financially supported by the National Key Research and Development Program of China (Grant No. 2023YFB2604800).These financial supports are gratefully acknowledged.was supported by the National Key Research and Development Program of China (SQ2023YFB2600225).

Declaration of competing interest

The authors have no competing interests to declare that are relevant to the content of this article.

Author contribution statement

Yu Jianhua: data curation, writing-review & editing, formal analysis. Quan Lei: conceptualization, methodology, software. Tian Bo: conceptualization, funding acquisition. Li Lihui: investigation. Zhang Panpan: methodology, software. Li Sili: funding acquisition, formal analysis.

Data availability statement

The original contributions presented in the study are included in the article, further inquiries can be directed to the corresponding author.

Use of AI statement

This study did not involve the use of artificial intelligence tools.

References

[1] Fang JH, Liu JK. Analysis of long-term changes for thermal regime of permafrost underlying subgrade along National Highway G214. China Journal of Highway and Transport, 2016, 29(11): 25–32.

[2] Wang SJ, Niu FJ, Chen JB, et al. Permafrost research in china related to express highway construction. Permafrost and Periglacial Processes, 2020, 31(3): 406–416.

[3] Zhou K, Tian B, Quan L, et al. Spatio-temporal evolution characteristics and influencing factors of permafrost underlying Gonghe-Yushu Expressway subgrade. Journal of Highway and Transportation Research and Development, 2024, 41(7): 40–48, 55.

[4] Qi JL, Sheng Y, Zhang JM, et al. Settlement of embankments in permafrost regions in the Qinghai-Tibet Plateau. Norsk Geografisk Tidsskrift - Norwegian Journal of Geography, 2007, 61(2): 49–55.

[5] Yu F, QI JL, Yao XL. Monitoring settlement at different depths within an embankment in permafrost region. Journal of Glaciology and Geocryology, 2011, 33(4): 813–818.

[6] Zhang JM, Liu D, Qi JL. Estimation on the settlement and deformation of embankment along Qinghai-Tibet Railway in permafrost regions. China Railway Science, 2007, 28(3): 12–17.

[7] Tian YH, Zhang QL, Mu YH, et al. Analysis on thawing consolidation and deformation of ground under earthen embankment in warm permafrost region. China Railway Science, 2014, 35(3): 1–7.

[8] Zhang QL, Li N, Ma W, et al. Analyses of the thawing consolidation of fill embankments in warm permafrost regions. Journal of Glaciology and Geocryology, 2014, 36(3): 614–621.

[9] Qi JL, Zhang JM, Yao XL, et al. Analysis of settlements of constructions in permafrost regions [J]. Rock and Soil Mechanics, 2009, 30(S2): 1–8.

[10] Wang SL. Permafrost degradation characteristics and foundation settlement prediction along Bei-Hei Expressway. Harbin: Northeast Forestry University, 2020.

[11] Ma QX, Fang JH. Influence of additional stress on the deformation mechanisms of embankment settlement. Highway, 2021, 66(3): 34–41.

[12] Yu K, Zhang JZ, Zhu DP. Analysis of deformation characteristics of embankment with deep permafrost table and degenerative permafrost. Rock and Soil Mechanics, 2013, 34: 3543–3548.

[13] Su K, Zhang JM, Liu SW, et al. Compressibility of warm and ice rich frozen soil. Journal of Glaciology and Geocryology, 2013, 35(2): 369–375.

[14] Ming F, Li DQ, Zhang Y. One dimensional thaw settlement of saturated frozen soil. Journal of Glaciology and Geocryology, 2016, 38(4): 1067–1073.

[15] Yang GS, Bai B, Yao XL. Study of thawing and consolidation law of ice-rich embankment. Rock and Soil Mechanics, 2020, 41(3): 1010–1018.

[16] Zhang H, Zhang JM, Zhang ZL, et al. Measurement of hydraulic conductivity of Qinghai-Tibet Plateau silty clay under subfreezing temperatures. Chinese Journal of Geotechnical Engineering, 2016, 38(6): 1030–1035.

[17] Liu SW, Zhang JM, Zhang H, et al. Preliminary discussion on pressure measurement of pore water in warm frozen soil. Journal of Gansu Agricultural University, 2011, 46(6): 155–160.

[18] Tian B. Highway foundation treatment techniques in permafrost regions of the Qinghai-Tibet Plateau: Current practices and future trends. Journal of Highway and Transportation Research and Development (English Edition), 2025, 19(3): 1–17.

[19] Bi GQ, Xiong M, Chai MT, et al. Experimental study on mechanical properties of undisturbed frozen soil on different depths in permafrost region. Journal of Lanzhou University of Technology, 2023, 49(3): 109–114.

[20] Chen J, Feng ZL, Sheng Y, et al. Permafrost along National Highway 214 and its engineering geological condition evaluation. Journal of Glaciology and Geocryology, 2014, 36(4): 790–801.

[21] Tian B, Wang HW, Quan L, et al. Risk assessment on surface deformation in permafrost area based on CPT test. Journal of Highway and Transportation Research and Development , 2023, 40(9): 1–7,53.

[22] Wang CD, Zhou SH, Wang BL, et al. Differential settlements in foundations under embankment load: Theoretical model and experimental verification. Geomechanics and Engineering, 2015, 8(2): 283–303.

[23] Yao HL, Cheng P, Wu WP. Prediction of ground heaves in expansive soils based on consolidation tests. Chinese Journal of Rock Mechanics and Engineering, 2005, 24(21): 3911–3915.

[24] Gao F, Zeng XZ, Zhong WH, et al. Progress and prospects of road engineering disease treatment technology in permafrost regions. Journal of China and Foreign Highway, 2024, 44(5): 1–16.

[25] Cheng J, Zhao XQ, Jin L, et al. Field test study on lime pile to treat foundation in island-shaped frozen soil. Journal of Railway Engineering Society, 2019, 36(1): 17–20,37.

[26] Wu LB, Qi W, Niu FJ, et al. A review of studies on roadbed frozen damage and countermeasures in seasonal frozen ground regions in China. Journal of Glaciology and Geocryology, 2015, 37(5): 1283–1293.

[27] Huang S R. Reinforcement of deep soft miscellaneous fill roadbed by high energy dynamic compaction replacement. Highway, 2023, 68(12): 71–76.

[28] Zhou K. Research on strong tamping consolidation technology for soft foundation in permafrost area. Beijing: Research Institute of Highway, Ministry of Transport, 2024.